

Dynamic analysis of three-mass vibratory system with twin crank-slider excitation mechanism

Vitaliy KORENDIY¹ , Volodymyr GURSKY¹ , Pavlo KROT² , Oleksandr KACHUR¹ 

¹ Lviv Polytechnic National University, S. Bandera Street 12, 79013 Lviv, Ukraine

² Wrocław University of Science and Technology, Wybrzeże Wyspiańskiego Street 27, 50-370 Wrocław, Poland,

Corresponding author: Vitaliy KORENDIY, email: vitaliy.nulp@gmail.com

Abstract The paper studies the dynamic behavior of the vibratory sieving conveyor equipped with the twin crank-slider excitation mechanism. The main purpose of this research consists in substantiating the possibilities of implementing the improved drive for providing the controllable vibration parameters of the working member (conveying tray, sieve, etc.) in accordance with the specific technological requirements set for different materials to be sieved and conveyed. In order to reach the goal set above, the following objectives are established: analyzing the design peculiarities of the vibratory sieving conveyor; deriving the mathematical model describing the conveyor's oscillatory system dynamic behavior; studying the system kinematic, dynamic, and power characteristics. The system motion is described using the Lagrange-d'Alembert principle, and the numerical modeling is carried out in the Mathematica software with the help of the Runge-Kutta methods. The influence of the vibratory system's geometrical parameters on the motion conditions of the conveyor's working member (conveying tray and sieve) is analyzed.

Keywords: vibratory conveyor, vibratory sieve, dynamic behavior, motion conditions, modeling.

1. Introduction

The vibratory equipment is widely used for sieving, screening, and conveying of various loose, bulky, and piecewise products. Among a great variety of vibration exciters, the inertial (unbalanced), electromagnetic, and crank-type ones are of the most commonly used in vibratory conveyors and screens. The problems of studying the dynamic behavior of vibratory machines equipped with different drives are of significant interest among scientists, technologists, and engineers all over the world.

The possibilities of providing the controllable elliptical oscillations of the vibratory screen by equipping it with two independent inertial exciters characterized by the changeable angular velocities are thoroughly analyzed in [1]. A similar vibration exciter with two coaxially rotating unbalanced masses set into motion by one electric motor is studied in [2]. The paper [3] is dedicated to investigating the dynamic behavior of the same coaxial double-mass exciter with two independent driving motors. The influence of different angular speed ratios of the kinematically synchronized unbalanced bodies on the dynamic behavior of the oscillatory system equipped with the doubled coaxial inertial vibration exciter is investigated in [4].

One more type of inertial vibration exciter equipped with passive auto-balancers is considered in the papers [5] and [6]. In [5], the authors studied the operational conditions of the three-mass anti-resonance vibratory machine controlled by changing both the unbalanced rotor speed and the forces of viscous resistance applied between the oscillating bodies. The paper [6] considers the dynamic behavior of the single-mass vibratory machine whose operation is based on the Sommerfeld effect.

A thorough analysis of different types of centrifugal (inertial) vibration exciters is carried out in [7], where the authors paid special attention to studying the dynamics of the asymmetric planetary vibration exciter. In [8], there is proposed a similar idea of developing the adjustable planetary vibration exciter with two satellite unbalanced rollers whose angular positions are synchronized by the chain gear. Another novel design of the directed vibration generating system equipped with the heavy eccentric pendulum-like mass being rotated and exciting the circular vibrations of the working member is studied in [9].

In distinction from the inertially driven machines considered in [1-9], the wide range of vibratory equipment uses the crank-type exciters [10-13]. The dynamics of the single-mass vibratory conveyor driven by the crank-and-rod vibration exciter is studied in [10]. A similar conveyor is considered in [11], where the author analyzed the dynamic parameters and the stress-strain state of the conveyor's hinges and rods. In [12], the authors investigated the translational locomotion of the semidefinite vibro-impact system

driven by the twin crank-slider exciter. The paper [13] is devoted to studying the kinematic characteristics of the shaking conveyor equipped with the crank-type vibration exciter.

The problems of the electric motor adjustment according to the operational conditions of the vibratory system with the rotating unbalanced mass are investigated in [14]. A similar problem is studied in [15], where the authors analyzed the dynamics of the single-degree-of-freedom reciprocating system driven by the DC motor and crank-slider mechanism. In addition, there are numerous investigations, e.g. [16], studying the possibilities of equipping various vibratory equipment with induction (asynchronous) motors with the corresponding control strategies. The basic aspects of predicting the safe fatigue life and failure diagnostics of the vibratory machines' springs are thoroughly investigated in [17].

The previous authors' investigations on similar problems dedicated to the development of the enhanced inertial vibration exciters are presented in [18–20]. The paper [18] is focused on studying the dynamics of the single-mass oscillatory system actuated by the asymmetric self-adjustable planetary-type vibration exciter. Similar designs of two excitation mechanisms of the symmetric structure are thoroughly studied in [19]. In addition, the possibilities of generating various trajectories of the single-mass vibratory system equipped with the proposed exciters are considered. The paper [20] investigates the kinematics of the controllable crank-type mechanism intended for actuating inertial or eccentric vibration exciters.

Unlike numerous scientific publications dedicated to studying the drive dynamics of various vibratory equipment, in particular those [1–20] considered above, the main idea of the present research consists in implementing the twin crank-slider mechanism for exciting oscillations of the vibratory sieving conveyor. The following investigations are aimed at substantiating the possibilities of providing multi-regime operational conditions that can be controlled in accordance with the specific technological requirements set for different materials to be sieved and conveyed. The practical implementation of the proposed ideas is presented in the developed general design of the vibratory sieving conveyor (see Fig. 1).

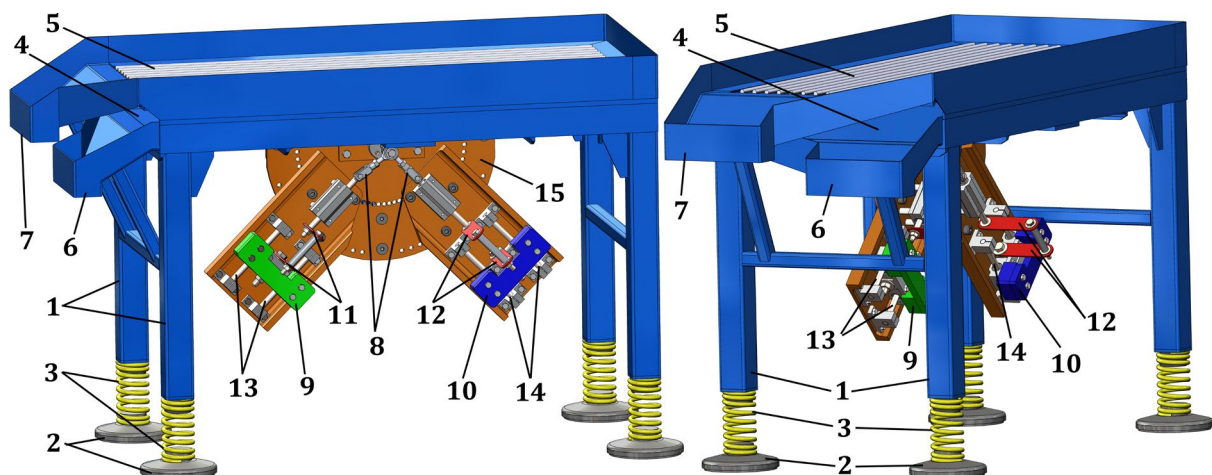


Figure 1. General design of the vibratory sieving conveyor.

The conveyor's body with four legs 1 is mounted on the foundation using the supports 2 and coil springs 3 (Fig. 1). The working member consists of the lower conveying tray 4 and the upper sieve 5, which have separate discharging holes 6 and 7, respectively. The vibrations are excited by the twin crank-slider mechanism 8 setting the disturbing bodies 9 and 10 into the rectilinear oscillatory motion with the help of the flat springs 11 and 12, respectively. The disturbing bodies 9 and 10 are equipped with the linear (pilot) bearings and slide along the corresponding guide rods 13, 14, whose angular positions with respect to the conveyor's body can be controlled. The whole exciter is mounted on the plate 15 fixed to the lower conveying tray 4. In order to reduce the parasitic angular oscillations, the intersection point of the disturbing bodies' guide axes must coincide with the mass center of the conveyor's body.

The main objectives of this research are the following: constructing the dynamic diagram of the conveyor's oscillatory system; deriving the differential equations describing the system motion; synthesizing the stiffness parameters providing the near-resonance vibrational conditions of the disturbing bodies and non-resonant (far-over-resonance) operation of the working member; analyzing the kinematic parameters of the vibratory system; studying the system's dynamic and power characteristics.

2. Research methodology

2.1. Dynamic diagram of the vibratory system

The conveyor's vibratory system consists of three movable bodies whose inertial parameters are characterized by the corresponding masses m_1 , m_2 , and m_3 (see Fig. 2). The working member (conveying tray, screen, or sieve) is set into the oscillatory motion due to the crank OA rotation providing the rectilinear vibrations of the masses m_2 and m_3 along the axes Ox_2 and Ox_3 , respectively. In order to restrict the angular oscillations of the mass m_1 the working member is elastically mounted on the movable platform using the independent vertical and horizontal spring-damper elements. The latter are characterized by the stiffness coefficients k_{1x} , k_{1y} , and damping coefficients c_{1x} , c_{1y} , respectively.

The considered vibratory system (see Fig. 2) is characterized by five degrees of freedom. The rectilinear motions of the oscillating masses m_2 and m_3 relative to the working member (mass m_1) are described by the corresponding coordinates x_2 and x_3 . The relative motion of the excitation mechanism is characterized by the angular position φ of the crank OA with respect to the horizontal axis Ox_1 . The vibrations of the working member are described by the corresponding horizontal and vertical displacements x_1 and y_1 . Therefore, the system motion can be uniquely modelled by five differential equations.

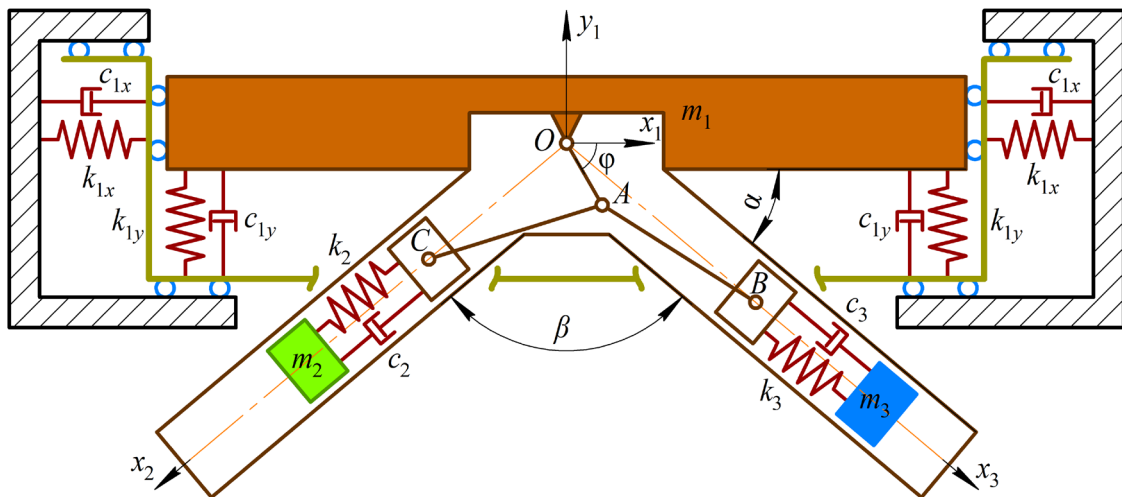


Figure 2. Dynamic diagram of the vibratory system.

2.2. Mathematical model describing the system motion

The differential equations describing the vibratory system motion were derived using the Lagrange-d'Alembert principle and can be presented as follows:

$$(m_1 + m_2 + m_3)\ddot{x}_1 + c_{1x}\dot{x}_1 + k_{1x}x_1 + k_2 \cos(\alpha + \beta) \cdot (x_{2C} - x_2) + k_3 \cos \alpha \cdot (x_{3B} - x_3) = -m_2\ddot{x}_2 \cos(\alpha + \beta) - m_3\ddot{x}_3 \cos \alpha; \quad (1)$$

$$(m_1 + m_2 + m_3)\ddot{y}_1 + c_{1y}\dot{y}_1 + k_{1y}y_1 + k_2 \sin(\alpha + \beta) \cdot (x_{2C} - x_2) + k_3 \sin \alpha \cdot (x_{3B} - x_3) = m_2\ddot{x}_2 \sin(\alpha + \beta) + m_3\ddot{x}_3 \sin \alpha; \quad (2)$$

$$m_2\ddot{x}_2 + c_2(\dot{x}_2 - \dot{x}_{2C}) + k_2(x_2 - x_{2C}) = m_2(\ddot{y}_1 \sin(\alpha + \beta) - \ddot{x}_1 \cos(\alpha + \beta)); \quad (3)$$

$$m_3\ddot{x}_3 + c_3(\dot{x}_3 - \dot{x}_{3B}) + k_3(x_3 - x_{3B}) = m_3(\ddot{y}_1 \sin \alpha - \ddot{x}_1 \cos \alpha); \quad (4)$$

$$J_0\ddot{\varphi} = T_{mot} - T_{load}, \quad (5)$$

where m_1, m_2, m_3 are the masses of the oscillating bodies, c_{1x}, c_{1y}, c_2, c_3 and k_{1x}, k_{1y}, k_2, k_3 are the damping and stiffness coefficients of the corresponding springs (see Fig. 2), α is the angle between the horizontal axis Ox_1 and the axis Ox_3 (the guideline of the slider B), β is the angle between the axes Ox_3 and Ox_2 (i.e., between the guidelines of the sliders B and C), x_{2C}, x_{3B} are the coordinates describing the relative positions of the corresponding sliders (C and B), J_0 is the equivalent moment of inertia reduced to the crank (motor) shaft, T_{mot}, T_{load} are the driving and loading torques applied to the crank (motor) shaft.

The relative positions of the sliders B and C can be described by the following dependencies:

$$x_{2C} = l_{OA} \cos(\alpha + \beta - \varphi) + \sqrt{l_{AC}^2 - (l_{OA} \sin(\alpha + \beta - \varphi))^2} \Big|_{l_{AC} \gg l_{OA}} \approx l_{OA} \cos(\alpha + \beta - \varphi) + l_{AC}; \quad (6)$$

$$x_{3B} = l_{OA} \cos(\alpha - \varphi) + \sqrt{l_{AB}^2 - (l_{OA} \sin(\alpha - \varphi))^2} \Big|_{l_{AB} \gg l_{OA}} \approx l_{OA} \cos(\alpha - \varphi) + l_{AB}, \quad (7)$$

where l_{OA} , l_{AC} , l_{AB} are the lengths of the corresponding rods of the excitation mechanism (see Fig. 2).

While performing further investigations, let us consider the simplified case of the system operation. This means that the crank angular velocity ω is assumed to be constant, and the differential equation (5) can be neglected. The considered simplifying assumption is valid in the cases of implementing the permanent-magnet direct-current motors characterized by high starting torque and equipped with the additional systems of speed or torque control [13, 14]. Therefore, the angular position φ of the crank OA with respect to the horizontal axis Ox_1 can be presented as a function of time: $\varphi = \omega \cdot t$.

2.3. Synthesis of the system parameters

The parametric synthesis of the considered vibratory system is aimed at providing the near-resonance vibrational conditions of the disturbing bodies (masses m_2 , m_3), and non-resonant (far-over-resonance) operation of the working member (mass m_1). Adopting the natural frequencies of the masses m_2 , m_3 almost equal to the forced frequency of the oscillatory systems, the stiffness parameters k_2 , k_3 of the corresponding springs (see Fig. 2) can be calculated as follows:

$$k_i = m_{1-i} \xi_i^2 \omega^2 + c_i^2 / (4m_{1-i}), \quad i = 2, 3, \quad (8)$$

where $m_{1-2} = m_1 m_2 / (m_1 + m_2)$, $m_{1-3} = m_1 m_3 / (m_1 + m_3)$ are the reduced (equivalent) masses of the corresponding spring systems (see Fig. 2), ξ_2 , ξ_3 are the correction coefficients providing the near-resonance vibrational conditions of the corresponding oscillating masses ($\xi_i = 0.95 \dots 0.99$).

Considering the fact that the working member (conveying tray, screen or sieve) is elastically mounted on the foundation using the independent vertical and horizontal spring-damper elements, the non-resonant (far-over-resonance) vibrational conditions must be provided to reduce the negative influence of the working member upon the foundation. In such a case, the corresponding stiffness coefficients k_{1x} , k_{1y} are to be determined using the following expressions:

$$k_{1j} = (m_1 + m_2 + m_3) \xi_{1j}^2 \omega^2 + c_{1j}^2 / (4(m_1 + m_2 + m_3)), \quad j = x, y, \quad (9)$$

where ξ_{1j} are the correction coefficients providing the far-over-resonance vibrational conditions of the working member ($\xi_{1j} = 0.15 \dots 0.4$).

3. Results and discussion

3.1. Analyzing the kinematic parameters of the vibratory system

While carrying out further numerical modeling of the vibratory system motion, let us adopt the following inertial and geometrical parameters based on the conveyor 3D-design (Fig. 1) developed in the SolidWorks software: $m_1 = 30$ kg, $m_2 = 1$ kg, $m_3 = 1$ kg, $l_{OA} = 0.015$ m, $l_{AB} = 0.08$ m, $l_{AC} = 0.08$ m. The operational parameters are the following: $\omega = 104.7$ rad/s (i.e., the motor shaft rotates at 1000 rpm), $c_{1x} = 100$ N·s/m, $c_{1y} = 100$ N·s/m, $c_2 = 50$ N·s/m, $c_3 = 50$ N·s/m. The stiffness coefficients are calculated by Eqs. (8) and (9) taking into account the corresponding correction coefficients $\xi_{1x} = 0.36$, $\xi_{1y} = 0.36$, $\xi_2 = 0.98$, $\xi_3 = 0.98$: $k_{1x} = 45400$ N/m, $k_{1y} = 45400$ N/m, $k_2 = 10800$ N/m, $k_3 = 10800$ N/m.

The angles α and β are considered as the basic parameters whose influence on the system's kinematics and dynamics is to be studied. Substituting the mentioned above values of the conveyor's geometrical, inertial, stiffness, and damping parameters in the system of the differential equations (1)–(4), the corresponding parametric solution (with the unknown parameters α and β) has been numerically derived in the Mathematica software using the Runge-Kutta methods. The latter are integrated into the Mathematica software by the "ExplicitRungeKutta" function allowing for solving stiff and quasi-stiff systems with the help of the proportional-integral step-size controller. The "ParametricNDSolve" function finds the numerical solution of the system of ordinary differential equations for the given functions (generalized coordinates) with the independent variable (time) in the prescribed range (e.g., 0...2 s) and with the changeable

parameters (angles α and β). The numerically obtained Figure 3 illustrates the trajectories of the working member vibrations at different values of α and β : $\alpha = 0^\circ, 30^\circ, \beta = 0^\circ, 30^\circ, 60^\circ, 90^\circ, 120^\circ, 150^\circ, 180^\circ$.

Due to changing the angle β , it is possible to provide rectilinear, elliptical, and circular oscillations of the working member. Rectilinear oscillations take place at $\beta = 0^\circ$ and $\beta = 180^\circ$; circular oscillations – at $\beta = 90^\circ$. All the other angles β provide elliptical oscillations of the working member (see Fig. 3). The change in the ellipse shape (focal distance, eccentricity, ratio between the minor and major axes, etc.) and the corresponding vibration parameters depend on the angle β value. In the case of $\alpha = 0^\circ$ (Fig. 3 a), the elliptical trajectories of the working member, allowing for the rightward conveying of different products, take place in the range of $0^\circ < \beta < 90^\circ$, while the leftward conveying can be provided at $90^\circ < \beta < 180^\circ$. In order to change the direction of the rectilinear vibrations, it is necessary to increase the angle α . For example, at $\alpha = 30^\circ$ (Fig. 3 b), the rectilinear vibrations and the major axes of the corresponding elliptical trajectories are counter-clockwise inclined at 30° with respect to their previous positions (at $\alpha = 0^\circ$). Therefore, the implementation of the controllable twin crank-slider excitation mechanism allows for changing the vibration parameters of the working member.

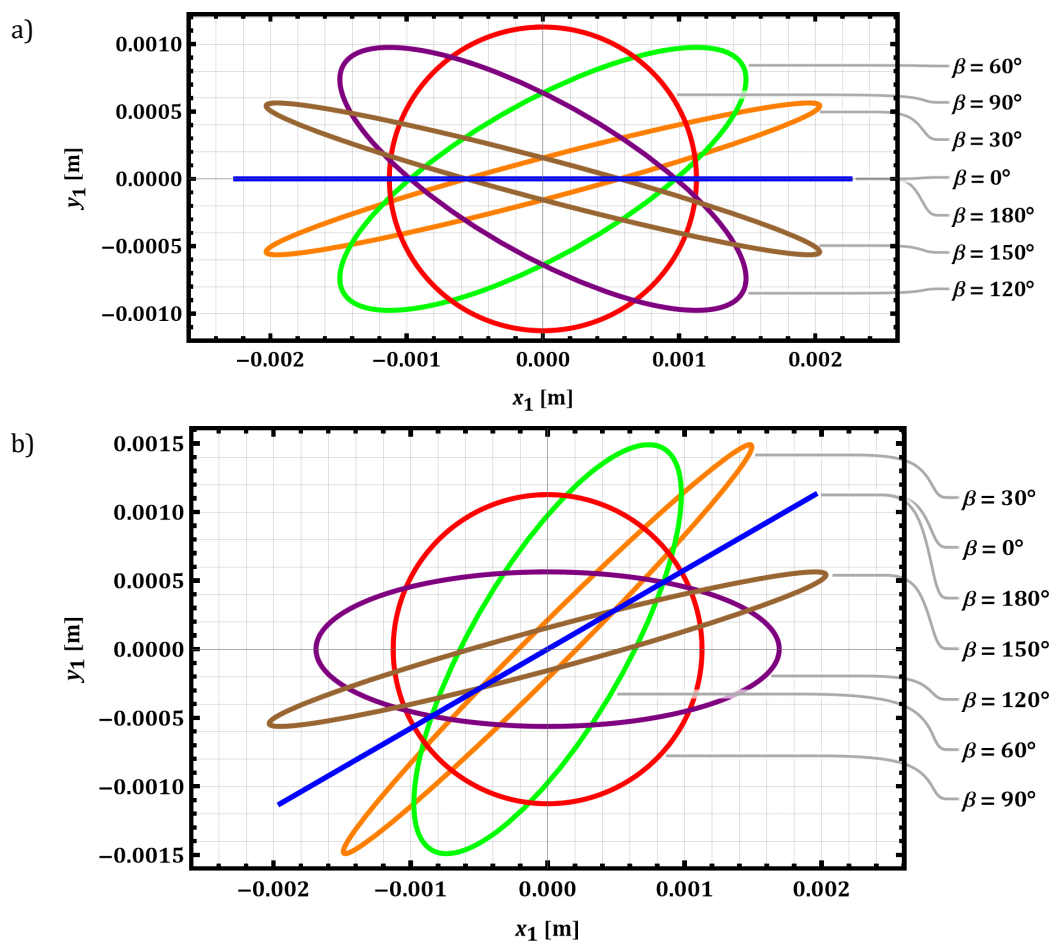


Figure 3. Trajectories of the working member vibrations at different values of α and β :
a) $\alpha = 0^\circ$, b) $\alpha = 30^\circ$.

Figure 4 presents the time response curves of the vibratory system's oscillating bodies at $\beta = 90^\circ$ and $\alpha = 0^\circ \dots 90^\circ$, i.e., under the conditions of the working member circular oscillations. Such operational conditions allow for providing the effective shaking and sieving processes of various loose and bulky products. The vibration amplitudes (x_{2amp} , x_{3amp}) of the disturbing bodies reach 35 mm, while the working member performs the circular oscillations characterized by the radius of about 1.2 mm, i.e., the phase shift between the vertical and horizontal oscillations of the working member equals $\pi/2$ rad. By means of changing the angles α and β , the trajectory shape of the working member can be controlled in accordance with the specific technological requirements set for different materials to be sieved and conveyed.

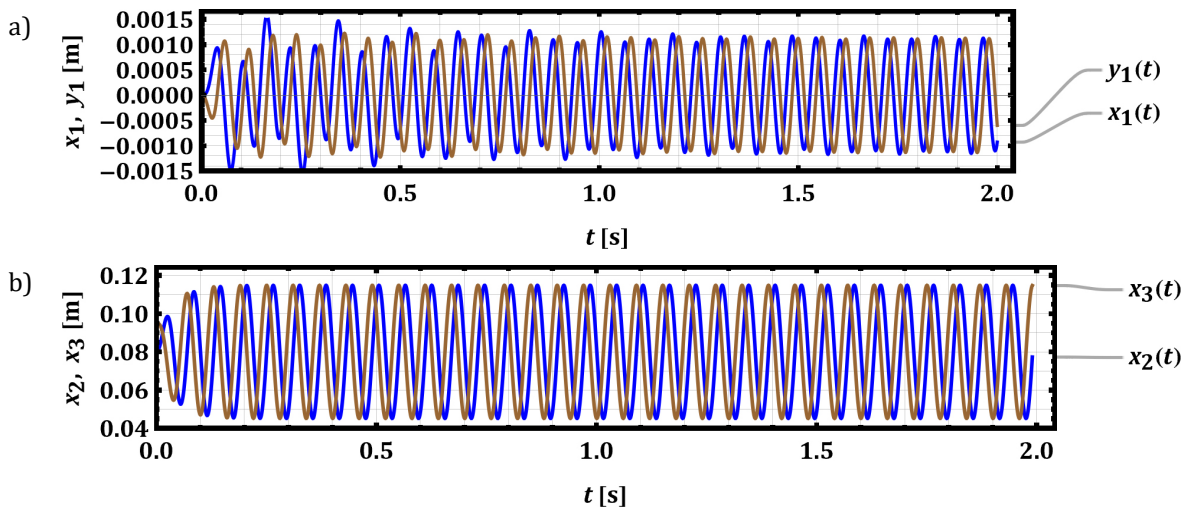


Figure 4. Time response curves of the corresponding oscillating masses at $\beta = 90^\circ$ and $\alpha = 0^\circ \dots 90^\circ$: a) working member (mass m_1), b) disturbing bodies (masses m_2, m_3).

As a second example, let us consider the system oscillations at $\alpha = 30^\circ$ and $\beta = 0^\circ$ (see Fig. 5), i.e., when the working member performs the directed (rectilinear) oscillations. In such a case, the effective conveying and sieving processes of various piecewise products can be provided. The amplitudes (x_{2ampl}, x_{3ampl}) of the disturbing bodies are about 35 mm, while the working member oscillates rectilinearly with the horizontal and vertical amplitudes of $x_{1ampl} = 2$ mm and $y_{1ampl} = 1.2$ mm, respectively. By means of changing the angle α , it is possible to control the throwing (pitching) angle of the working member (conveying tray and sieve) in order to improve the sieving and conveying efficiency for different piecewise and bulky products.

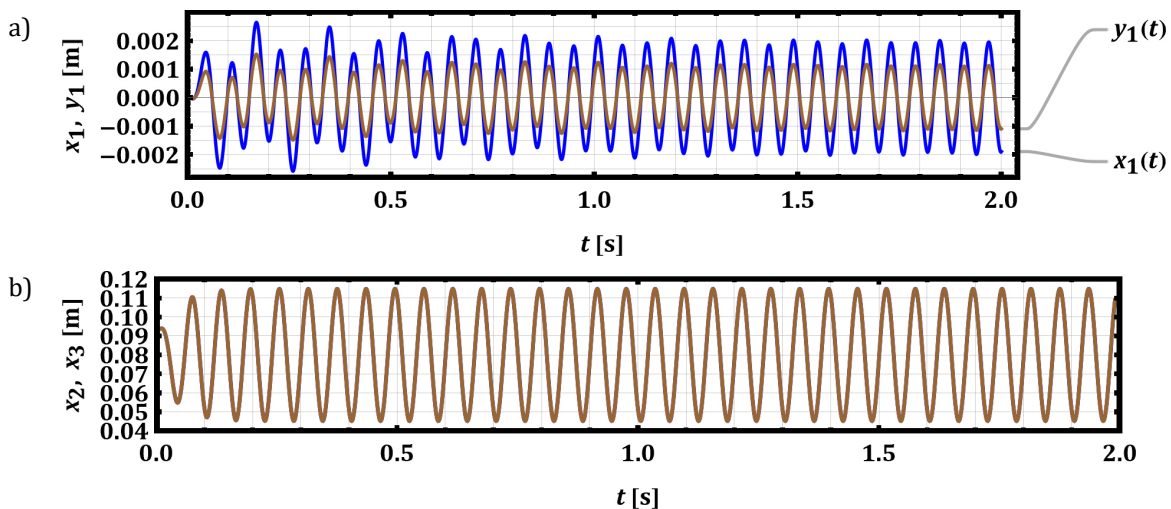


Figure 5. Time response curves of the corresponding oscillating masses at $\alpha = 30^\circ$ and $\beta = 0^\circ$: a) working member (mass m_1), b) disturbing bodies (masses m_2, m_3).

3.2. Studying the dynamic and power characteristics

The second stage of the present research consists in the following tasks: analyzing the working member vertical acceleration and vibration intensity factor (Fig. 6); studying the drive loading torque (Fig. 7) and power consumption under different operational conditions. Considering the case when $\alpha = 0^\circ$ (Fig. 6 a), the largest values of the vibration intensity factor (W) and vertical acceleration (\ddot{y}_1) of the working member take place at $\beta = 90^\circ$ (circular oscillations) and reach 1.25 and 12.5 m/s^2 , respectively.

Under the conditions of $\alpha = 30^\circ$ (Fig. 6 b), the working member vertical acceleration and vibration intensity factor take the amplitude values of about 17 m/s^2 and 1.7, respectively, at $\beta = 30^\circ$ and $\beta = 60^\circ$ (elliptical oscillations). In the case when $\alpha = 30^\circ, \beta = 90^\circ$ (circular oscillations), the considered dynamic characteristics of the working member vibrations are similar to the ones obtained for $\alpha = 0^\circ, \beta = 90^\circ$.

Therefore, it can be stated that the proposed twin crank-slider excitation mechanism allows for changing the vibratory conveyor dynamic parameters in accordance with the specific technological requirements set for different materials to be sieved and conveyed.

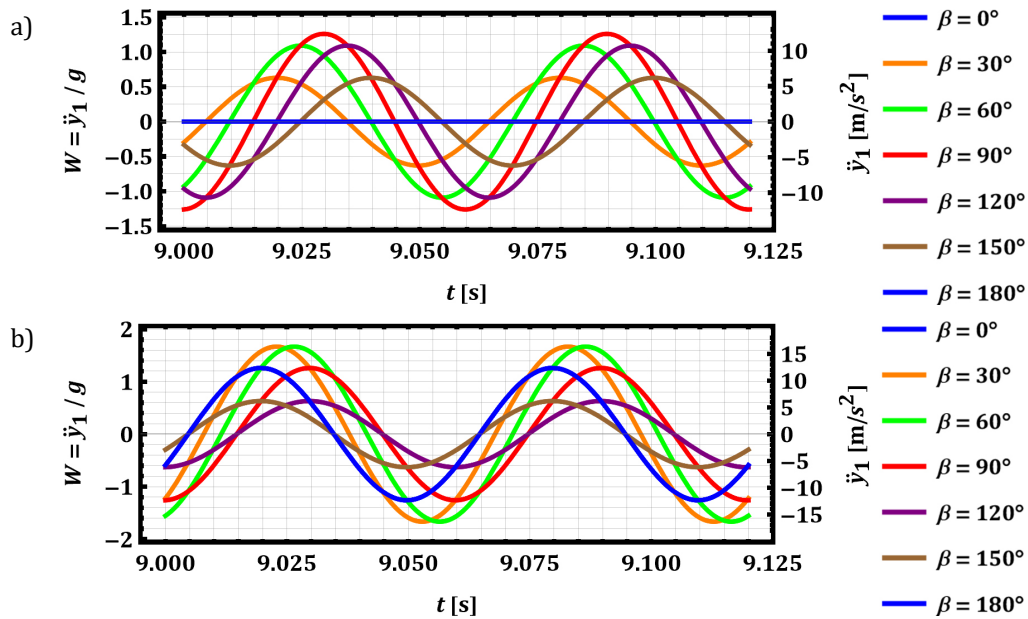


Figure 6. Time dependencies of the working member vibration intensity factor and vertical acceleration at different values of α and β : a) $\alpha = 0^\circ$, b) $\alpha = 30^\circ$.

The equivalent loading torque applied to the crank (motor) shaft is proportional to the restoring forces of the disturbing bodies' springs and can be calculated using the following simplified expression:

$$T_{load} \approx (m_2g \sin(\alpha + \beta) + k_2(x_2 - x_{2C}))l_{OA} \sin(\varphi - \alpha - \beta) + (m_3g \sin(\alpha) + k_3(x_3 - x_{3B}))l_{OA} \sin(\varphi - \alpha), \tag{10}$$

where g is the free fall (gravitational) acceleration.

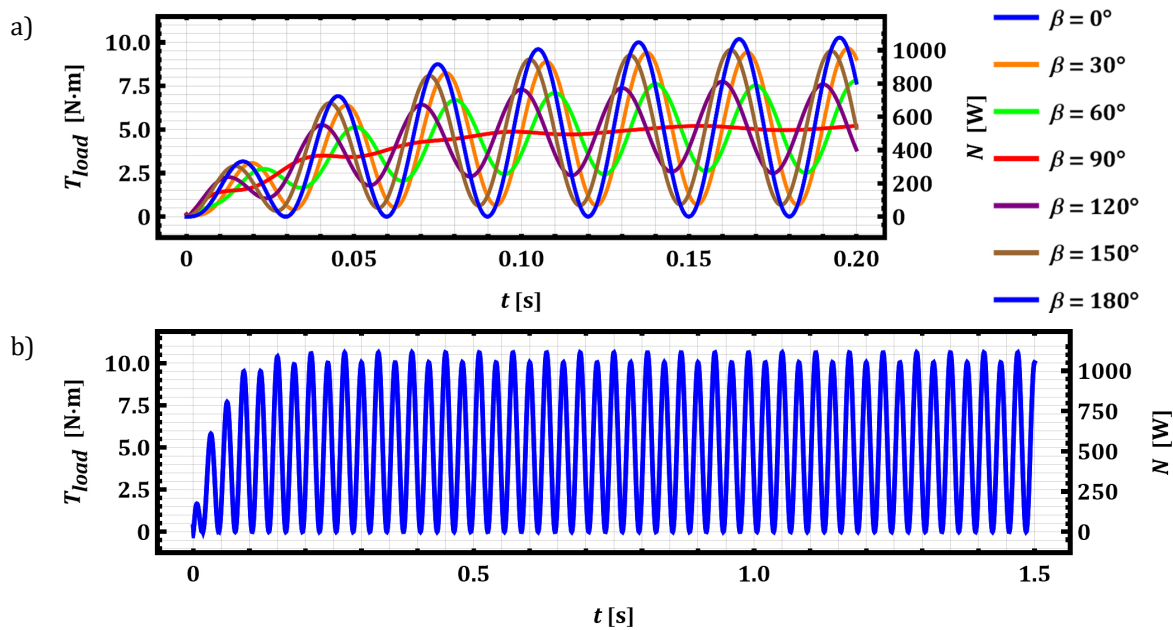


Figure 7. Time dependencies of the loading torque applied to the crank (motor) shaft at different values of α and β : a) $\alpha = 0^\circ, \beta = 0^\circ \dots 180^\circ$, b) $\alpha = 90^\circ, \beta = 0^\circ$.

The results of the loading torque numerical modeling carried out in the Mathematica software using Eq. (10) are presented in Fig. 7. In the hardest (extreme) operational conditions (when $\alpha = 90^\circ$, $\beta = 0^\circ$, i.e., the working member performs vertical rectilinear oscillations at the amplitude of 2.2 mm and the acceleration of 25 m/s²), the maximal loading torque reaches 11 N·m, while its minimal value is zero. The average value of the torque was calculated as $T_{load.av} = \frac{\omega}{2\pi} \int_{t_1}^{t_1+2\pi/\omega} T_{load} dt$ and is about 5.2 N·m.

The maximal and minimal instantaneous values of the loading power ($N = \omega T_{load}$) are about 1100 W and 0 W (Fig. 7). The average power consumption was calculated as $N_{av.} = \frac{\omega^2}{2\pi} \int_{t_1}^{t_1+2\pi/\omega} T_{load} dt$ under different operational conditions. In the hardest (extreme) operational conditions considered above (i.e., $\alpha = 90^\circ$, $\beta = 0^\circ$), the average power needed to be supplied by the conveyor's drive is equal to 540 W.

4. Conclusions

The paper considers the improved design of the vibratory sieving conveyor equipped with the twin crank-slider excitation mechanism (Fig. 1). The implementation of such a drive provides the possibility of controlling the vibration parameters of the working member in accordance with the technological requirements set for different loose, bulky, and piecewise products to be sieved and conveyed. Based on the dynamic diagram of the conveyor's oscillatory system (Fig. 2), the mathematical model describing the system motion was derived (Eqs. (1)-(7)). The analytical expressions for determining the stiffness parameters of the corresponding springs of the vibratory system were deduced (Eqs. (8) and (9)) based on the assumptions of providing the near-resonance vibrational conditions of the disturbing bodies (masses m_2 , m_3) and non-resonant (far-over-resonance) operation of the working member (mass m_1).

The numerical modelling of the conveyor operation was carried out at different values of the angles α and β defining the vibration directions of the disturbing bodies (see Fig. 2). The conditions of providing the rectilinear (directed), elliptical, and circular oscillations of the conveyor's working member were analyzed (see Figs. 3, 4, and 5), and its vertical acceleration and vibration intensity factor were studied (see Fig. 6). The loading torque applied to the crank (motor) shaft and the corresponding power consumption of the conveyor's drive were calculated under different operational conditions (circular, elliptical, horizontal, inclined, and vertical rectilinear oscillations) of the working member (see Fig. 7).

Additional information

The authors declare no competing financial interests and that all material taken from other sources (including their own published works) is clearly cited and that appropriate permits are obtained.

References

1. B. Chen, J. Yan, Z. Yin, K.K. Tamma; A new study on dynamic adjustment of vibration direction angle for dual-motor-driven vibrating screen; Proceedings of the Institution of Mechanical Engineers, Part E: Journal of Process Mechanical Engineering, 2021, 235(2), 186–196; DOI: 10.1177/0954408920952603
2. V. Gursky, I. Kuzio, P. Krot, R. Zimroz; Energy-saving inertial drive for dual-frequency excitation of vibrating machines; Energies, 2021, 14(1), 14010071; DOI: 10.3390/en14010071
3. V. Gursky, P. Krot, V. Korendiy, R. Zimroz; Dynamic analysis of an enhanced multi-frequency inertial exciter for industrial vibrating machines; Machines, 2022, 10(2), 10020130; DOI: 10.3390/machines10020130
4. V. Gursky, V. Korendiy, P. Krot, R. Zimroz, O. Kachur, N. Maherus; On the dynamics of an enhanced coaxial inertial exciter for vibratory machines; Machines, 2023, 11(1), 97; DOI: 10.3390/machines11010097
5. V. Yatsun, G. Filimonikhin, V. Pirogov, V. Amosov, P. Luzan; Research of anti-resonance three-mass vibratory machine with a vibration exciter in the form of a passive auto-balancer, Eastern-European Journal of Enterprise Technologies, 2020, 5(7(107)), 89–97; DOI: 10.15587/1729-4061.2020.213724
6. G. Filimonikhin, V. Pirogov, M. Hodunko, R. Kisilov, V. Mazhara; The dynamics of a resonance single-mass vibratory machine with a vibration exciter of targeted action that operates on the Sommerfeld effect; Eastern-European Journal of Enterprise Technologies, 2021, 3(7(111)), 51–58; DOI: 10.15587/1729-4061.2021.233960
7. A. Kim, M. Doudkin, A. Ermilov, G. Kustarev, M. Sakimov, M. Mlynczak; Analysis of vibroexciters working process of the improved efficiency for ice breaking, construction and road machines; Journal of Vibroengineering, 2020, 22(3), 465–485; DOI: 10.21595/jve.2020.20446

8. V.V. Mikheyev, S.V. Saveliev; Planetary adjustable vibratory exciter with chain gear; *Journal of Physics: Conference Series*, 2019, 1210(1), 012097; DOI: 10.1088/1742-6596/1210/1/012097
9. V.V. Mikheyev; New type of vibration generator with vibratory force oriented in preferred direction; *Journal of Vibration Engineering and Technologies*, 2018, 6(2), 149–154; DOI: 10.1007/s42417-018-0025-4
10. G.F. Alşverişçi; The nonlinear behavior of vibrational conveyers with single-mass crank-and-rod exciters; *Mathematical Problems in Engineering*, 2012, 534189; DOI: 10.1155/2012/534189
11. Z. Algazy; The substantiating of the dynamic parameters of the shaking conveyor mechanism; *Vibroengineering Procedia*, 2015, 5, 15–20.
12. V. Korendiy, V. Gursky, O. Kachur, V. Gurey, O. Havrylchenko, O. Kotsiumbas; Mathematical modeling of forced oscillations of semidefinite vibro-impact system sliding along rough horizontal surface; *Vibroengineering Procedia*, 2021, 39, 164–169; DOI: 10.21595/vp.2021.22298
13. V. Korendiy, O. Kachur, P. Dmyterko; Kinematic analysis of an oscillatory system of a shaking conveyor-separator; In: *Advanced Manufacturing Processes III. InterPartner 2021. Lecture Notes in Mechanical Engineering*; V. Tonkonogyi, V. Ivanov, J. Trojanowska, G. Oborskyi, I. Pavlenko, Eds.; Springer: Cham, Switzerland, 2022, 592–601; DOI: 10.1007/978-3-030-91327-4_57
14. A. Bisoi, A.K. Samantaray, R. Bhattacharyya; Control strategies for DC motors driving rotor dynamic systems through resonance; *Journal of Sound and Vibration*, 2017, 411, 304–327; DOI: 10.1016/j.jsv.2017.09.014
15. A. Sinha, S.K. Bharti, A.K. Samantaray, G. Chakraborty, R. Bhattacharyya; Sommerfeld effect in an oscillator with a reciprocating mass; *Nonlinear Dynamics*, 2018, 93(3), 1719–1739; DOI: 10.1007/s11071-018-4287-x
16. M.P. Yaroshevich, I.P. Zabrodets, T.S. Yaroshevich; Dynamics of vibrating machines starting with unbalanced drive in case of bearing body flat vibrations; *Naukovyi Visnyk Natsionalnoho Hirnychoho Universytetu*, 2015, 3, 39–45.
17. P. Krot, R. Zimroz, A. Michalak, J. Wodecki, Sz. Ogonowski, M. Drozda, M. Jach; Development and verification of the diagnostic model of the sieving screen; *Shock and Vibration*, 2020, 8015465; DOI: 10.1155/2020/8015465
18. V. Korendiy, I. Kuzio, S. Nikipchuk, O. Kotsiumbas, P. Dmyterko; On the dynamic behavior of an asymmetric self-regulated planetary-type vibration exciter; *Vibroengineering Procedia*, 2022, 42, 7–13; DOI: 10.21595/vp.2022.22580
19. V. Korendiy, V. Gurey, V. Borovets, O. Kotsiumbas, V. Lozynskyy; Generating various motion paths of single-mass vibratory system equipped with symmetric planetary-type vibration exciter; *Vibroengineering Procedia*, 2022, 43, 7–13; DOI: 10.21595/vp.2022.22703
20. O. Lanets, O. Kachur, V. Korendiy, V. Lozynskyy; Controllable crank mechanism for exciting oscillations of vibratory equipment; In: *Advances in Design, Simulation and Manufacturing IV. DSMIE 2021. Lecture Notes in Mechanical Engineering*; V. Ivanov, I. Pavlenko, O. Liaposhchenko, J. Machado, M. Edl, Eds.; Springer: Cham, Switzerland, 2021, 43–52; DOI: 10.1007/978-3-030-77823-1_5

© 2023 by the Authors. Licensee Poznan University of Technology (Poznan, Poland). This article is an open access article distributed under the terms and conditions of the Creative Commons Attribution (CC BY) license (<http://creativecommons.org/licenses/by/4.0/>).